

Ratio of forbidden transition rates in the ground-state configuration of O II

Xiao-Ying Han,^{1,*} Xiang Gao,² De-Ling Zeng,³ Jun Yan,¹ and Jia-Ming Li^{4,5}

¹Data Center for High Energy Density Materials, Institute of Applied Physics and Computational Mathematics, Beijing 100088, China

²Beijing Computational Science Research Center, Beijing 100084, China

³Institute of Atomic and Molecular Physics, Jilin University, Changchun 130012, China

⁴Key Laboratory for Laser Plasma (Ministry of Education) and Department of Physics, Shanghai Jiao Tong University, Shanghai 200240, China

⁵Department of Physics and Center for Atomic and Molecular Nanosciences, Tsinghua University, Beijing 100084, China

(Received 23 February 2012; published 7 June 2012)

Based on a set of “quasicomplete bases,” using the large-scale multiconfiguration Dirac-Fock (MCDF) method, we calculate the forbidden electric quadrupole ($E2$) and magnetic dipole ($M1$) transition rates of the transitions ${}^2D_{5/2,3/2}^o \rightarrow {}^4S_{3/2}^o$ of the O II ground state considering the quantum electrodynamics (QED) corrections. Our calculations demonstrate that the Breit interactions are most important among all the QED corrections. The calculated $E2$ and $M1$ transition rates converge in a systematical and uniform manner with the extending orbital basis and the calculation uncertainty of 2.5% is achieved by considering the valence- and core-excitation correlations totally. With the converged transition rates, a value of the intensity ratio between the two transitions in high-electron-density limit in planetary nebulas is given, that is, $r(\infty) = 0.363 \pm 0.009$, which is within the overlap of the different observations and with the least uncertainty up to now. In addition, the $E2$ and $M1$ transition rates of two transitions ${}^2P_{3/2,1/2}^o \rightarrow {}^4S_{3/2}^o$ of O II ground state and the ratio between the two transition rates in high-electron-density limit are calculated and compared with the previous results.

DOI: 10.1103/PhysRevA.85.062506

PACS number(s): 32.10.-f, 32.70.-n, 95.30.Ky

I. INTRODUCTION

Oxygen is one of the abundant elements in astronomy and astrophysics. In planetary nebulas (PNs), the ratio between the two transitions ${}^2D_{5/2,3/2}^o \rightarrow {}^4S_{3/2}^o$ of O II ground state [$1s^2 2s^2 2p^3$], that is, $I(3729)/I(3726)$, is used to diagnose the electron densities [1]. In the high-electron-density limit, the detailed balance between the collisional excitations and deactivations produces a Boltzmann distribution of the ionic states. The line intensities are proportional to the radiative transition rates and the static weights of the ionic states when the split of ${}^2D_{5/2,3/2}^o$ states is much lower than the electron temperature of the PNs. In low-electron-density limit, the line intensities are proportional to the collision strengths because of the equilibrium between the radiative transitions and the collisional excitations. This paper mainly focuses on the intensity ratio in high-electron-density limit.

The transitions ${}^2D_{5/2,3/2}^o \rightarrow {}^4S_{3/2}^o$ of O II ground state [$1s^2 2s^2 2p^3$] are forbidden for electric dipole ($E1$) radiations; hence, the total transition rates are mainly determined by electric quadrupole ($E2$) and magnetic dipole ($M1$) radiations, about which some studies [2–5] have been carried out. More specifically, Eissner and Zeippen [2] investigated the importance of the two-electron Breit terms (within the Breit-Pauli approximation) on the $M1$ transition rates of O II; Fisher and Tachiev [3–5] investigated the extensive correlation effects and the importance of the core-excitation correlations in $E1$, $E2$, and $M1$ transition rates through a nonrelativistic multi-configuration Hartree-Fock (MCHF) calculation followed by a configuration interaction (CI) calculation using the Breit-Pauli (BP) Hamiltonian. Chen *et al.* [6] calculated the $E2$ and $M1$

transition rate of ${}^2D_{5/2,3/2}^o \rightarrow {}^4S_{3/2}^o$ transitions of O II ground state through a MCDF calculation. In Chen’s calculation, the core-excitation correlations are not considered in their CI calculation and the convergence of these two forbidden transition rates is not uniform. In this work, we use a GRASP-JT code, which is based on the GRASP2K code [7] to carry out a “quasicomplete basis” scenario demonstrated in the previous work [8], to calculate the $E2$ and $M1$ transition rates of O II ground state. Our calculations are fully relativistic and take into account of the large-scale electron correlations (including the valence- and core-excitation correlations) based on a set of quasicomplete basis and include the quantum electrodynamic (QED) corrections as perturbations. Adopting the quasicomplete basis scenario can fully utilize the variational principle; for example, the convergence of the present results is in a more systematical and uniform manner than Chen’s calculation. Our calculated $E2$ and $M1$ transition rates converge uniformly with an uncertainty of about 2.5%. With the converged $E2$ and $M1$ transition rates, a value for the intensity ratio in the limit of high electron density, that is, $r(\infty) = 0.363 \pm 0.009$, is given. This value is within the overlap of the astronomical observations by Wang *et al.* [9], Monk *et al.* [10], and Copetti and Writzel [11] and is more accurate than other theoretical results [1,6,12–14]. Furthermore, the forbidden $E2$ and $M1$ transition rates of the other two transitions ${}^2P_{3/2,1/2}^o \rightarrow {}^4S_{3/2}^o$ of O II ground state and the ratio between the two transition rates in high-electron-density limit are calculated and compared with the other results [4].

II. THEORY

A brief description of the MCDF method will be presented here. The interactions in a many-electron atomic system can be separated into two sorts: longitudinal and transverse

*han_xiaoying@iapcm.ac.cn

interactions. In the Coulomb gauge, the atomic Hamiltonian only with the longitudinal electron-nucleus and electron-electron interactions, can be expressed as (atomic units are used throughout the paper if not specified)

$$H_{DC} = \sum_i \left[c\vec{\alpha} \cdot \vec{p}_i + (\beta + 1)c^2 - \frac{Z}{r_i} \right] + \sum_{i < j} \frac{1}{r_i - r_j}. \quad (1)$$

The transverse interactions and the interactions with radiation fields are treated as perturbations. The full relativistic atomic orbital (AO) wave functions are obtained by solving the Dirac-Fock equations self-consistently, that is,

$$H_{DC}\Psi = E\Psi. \quad (2)$$

In this work we use a GRASP-JT code, which is based on GRASP2K code [7] to carry out a quasicomplete basis scenario [8], to calculate all the relevant AO bases. More specifically, the AOs with principal quantum numbers $n = 1, 2$ are optimized together by multiconfiguration self-consistent-field (MCSCF) iterations to minimize the statistic weight summation \mathcal{F} of the lowest five energy levels $^4S_{3/2}^o, ^2D_{5/2,3/2}^o, ^2P_{3/2,1/2}^o$ of O II ground state [$1s^2 2s^2 2p^3$]. Here the multiconfigurations are generated by single (\mathcal{S}) and double (\mathcal{D}) electron excitations from the reference configuration $1s^2 2s^2 2p^3$. The AOs with $n = 1, 2$ are spectral orbital bases with $n - l - 1$ nodes. Then the AOs with $n = 1, 2$ are fixed, and the AOs with $n = 3$ are obtained by MCSCF iterations to optimize the same \mathcal{F} , where the configurations are generated by \mathcal{S} and \mathcal{D} electron excitations from the reference configurations $2p^3$ and $2p^2 3p$ to all the AOs with $n = 2, 3$ and $l = 0, \dots, n - 1$ (namely, the occupation number of $1s$ orbital of all the configurations is fixed to be 2). In succession, with the AOs ($n \leq 3$) fixed, the AOs are extended to $n_{\max} = 4, \dots, 9$ from n to $n + 1$ by optimizing \mathcal{F} with the multiconfigurations generated by \mathcal{S} and \mathcal{D} electron excitations from the reference configurations $2p^3$ and $2p^2 3p$ to the AOs with $n = 2, \dots, n_{\max}$ and $l = 0, \dots, \min(n_{\max} - 1, 7)$. All the nodes of AOs with $n \geq 3$ are not fixed and they are expected to be pseudostate orbitals.

Configuration state functions (CSFs) are linear combinations of Slater determinations of the AOs with $n \leq n_{\max}$. Atomic state functions (ASFs) are linear combinations of CSFs with the same parity (P), total angular momentum (J), and

magnetic quantum number (M), which can be expressed as

$$|\Gamma P J M; n_{\max}\rangle = \sum_{r=1}^{n_c} C_{r\Gamma} |\gamma_r P J M; n_{\max}\rangle, \quad (3)$$

where $C_{r\Gamma}$ is the mixing coefficient and Γ, γ represent all other quantum numbers. The energy levels are calculated by CI method including the \mathcal{S} and \mathcal{D} electron excitations configurations from the reference configuration $1s^2 2s^2 2p^3$, which means the core ($1s^2$) and valence ($2s^2 2p^3$) are all relaxed. So the CI calculations take account of all the valence- and core-excitation correlations, which are important for convergence. The QED corrections, especially the Breit interaction, are added to the atomic Hamiltonian as a perturbation in the CI calculations. The Breit interaction is the most important high-order correction not only for the energy levels but also for the transition rates. The Breit (transverse) interaction represents the relativistic retardation effect of electromagnetic interactions with the finite velocity of light [15, 16], especially the retarded magnetic interactions among the electron currents [17], which are illustrated later by the calculation results.

Table I shows our calculated lowest five energy levels and the fine structure splits of O II ground state based on AOs with $n_{\max} = 9$ ($l \leq 7$), taking account of the Breit interaction and the comparisons with other theoretical and experimental values. Our calculated fine structure energy levels, especially the $^2D_{5/2,3/2}^o$ energy levels, are in good agreement with the experimental values. Our calculated fine structure splits also agree well with the experimental values. The other theoretical results [3, 4, 6] all agree well with the experimental values, especially the results of Fisher and Tachiev [4] being the same with the experimental values. The results of Fisher and Tachiev [3, 4] are calculated through a MCHF + BP calculation. Chen *et al.*'s [6] results are from a MCDF calculation, which differ from our calculations in two ways: (1) In their calculations, the AOs with $n \leq 5$ are prepared with core ($1s^2$) relaxed and the AOs with $n = 6, 7$ are prepared with core ($1s^2$) frozen, while our all AOs are prepared with core ($1s^2$) frozen except the AOs with $n = 1, 2$; (2) in Chen's CI calculations the core $1s^2$ is frozen and the number of CSFs of three J^π symmetries are 7970 for $J^\pi = 1/2^-$, 14 208 for $J^\pi = 3/2^-$, 17 599 for $J^\pi = 5/2^-$, while in our CI calculations the core $1s^2$ is relaxed

TABLE I. The fine structure energy levels and fine structure splits of O II ground state [$1s^2 2s^2 2p^3$] (in atomic units).

Term	This work ($n_{\max} = 9$)	Expt. ^a	Δ^b	Chen ^c ($n_{\max} = 7$)	Δ	Tachiev and Fisher ^d	Δ	Fisher and Tachiev ^e
$^4S_{3/2}^o$	0	0		0		0		0
$^2D_{5/2}^o$	0.122 865	0.122 158	0.58%	0.122 850	0.57%	0.123 129	0.79%	0.122 158
$^2D_{3/2}^o$	0.122 957	0.122 249	0.58%	0.122 941	0.57%	0.123 219	0.79%	0.122 248
$^2D_{3/2}^o - ^2D_{5/2}^o$	-0.000 091	-0.000 091		-0.000 091		-0.000 090		-0.000 090
$^2P_{3/2}^o$	0.186 285	0.184 384	1.03%	0.184 793	0.22%	0.184 877	0.27%	0.184 386
$^2P_{1/2}^o$	0.186 293	0.184 393	1.03%	0.184 806	0.22%	0.184 889	0.27%	0.184 398
$^2P_{3/2}^o - ^2P_{1/2}^o$	-0.000 008	-0.000 009		-0.000 012		-0.000 012		-0.000 012

^aExperiment by Wenåker [18].

^bPercentage difference between the calculations and the experimental values [18].

^cCalculations by Chen [6].

^dCalculations by Tachiev and Fischer [3].

^eCalculations by Fischer and Tachiev [4].

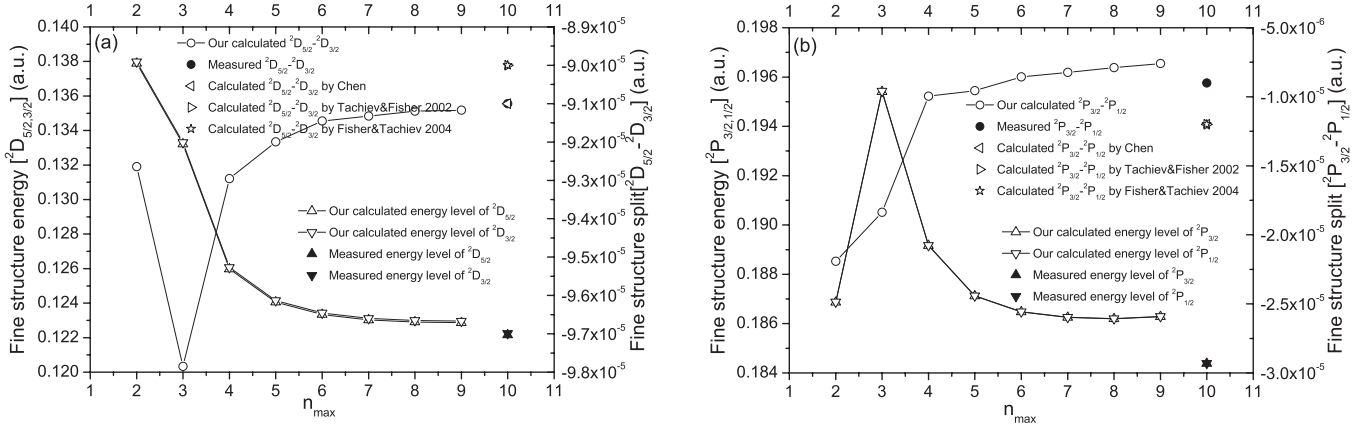


FIG. 1. Our calculated fine structure energy levels and fine structure splits of ${}^2D_{5/2,3/2}^o$ and ${}^2P_{3/2,1/2}^o$ states converge with the increasing n_{\max} of the AO bases. Results of ${}^2D_{5/2,3/2}^o$ states are shown in panel (a) and results of ${}^2P_{3/2,1/2}^o$ states are shown in panel (b). Our calculation results consider the Breit interaction. In addition, the measured [18] and other theoretical [3,6] values are plotted for comparison.

and the number of CSFs of three J^π symmetries are 59 684 for $J^\pi = 1/2^-$, 108 649 for $J^\pi = 3/2^-$, 139 620 for $J^\pi = 5/2^-$. The calculated energy levels of Chen are a little better than our calculations. However, in the following we see that their calculated two $E2$ transition rates of ${}^2D_{5/2,3/2}^o \rightarrow {}^4S_{3/2}^o$ do not converge uniformly, which brings a bigger uncertainty of the total transition rates than our results.

Figure 1 shows the convergence process of our calculated fine structure energy levels and splits with the increasing n_{\max} . In Fig. 1, an inconsistent variation of the convergence process is shown at $n_{\max} = 3$ of the curves for the fine structure splits of ${}^2D_{5/2,3/2}^o$ states [in panel (a)] and the fine structure levels of ${}^2P_{3/2,1/2}^o$ states [in panel (b)]. It is noted that the AOs of $n_{\max} = 2$ are spectral orbitals, while the AOs of $n_{\max} = 3$ begin to be pseudostate orbitals. Therefore, the inconsistent feature at $n_{\max} = 3$ should result from the break feature of the AO bases. After $n_{\max} = 3$, the convergence shows a systematical and uniform manner with the extending bases.

The spontaneous radiative transition rate for a discrete transition $i \rightarrow j$ can be obtained as

$$A_{ij} = \frac{2\pi}{2J_i + 1} \sum_{M_i, M_j} |\langle \Gamma_j P_j J_j M_j | T_\lambda^{(k)} | \Gamma_i P_i J_i M_i \rangle|^2, \quad (4)$$

where $T_\lambda^{(k)}$ is the multipole radiation field operator. According to the Wigner-Eckart theorem, the transition matrix element is related to the reduced matrix element $\langle \Gamma_j P_j J_j M_j | T_\lambda^{(k)} | \Gamma_i P_i J_i M_i \rangle$. Substituting the ASFs with CSFs, and in turn with AOs, the reduced matrix element can be calculated by the sum of single-electron reduced matrix elements. In the Coulomb gauge, $T^{(k)}$ has two forms: $T^{(k)}(m)$ for magnetic fields and $T^{(k)}(e)$ for electric fields. The Coulomb gauge corresponds to the velocity form in the nonrelativistic limit. For the length form, the electric multipole operator has another form $T^{(k)}(e) = T^{(k)}(e) + \sqrt{(k+1)/k} T_l^{(k)}(e)$. The details are described elsewhere [19–21].

In the MCDF method, if the wave functions are accurate the electric transition rates calculated in length and velocity forms should be the same. However, the results in two forms are usually different in multiconfiguration calculations since

the wave functions do not converge completely. Therefore, the convergence of the values in two forms provides a stringent test for the accuracy of the wave functions. In the velocity form, the reduced matrix element $\langle \Gamma_j P_j J_j M_j | T_\lambda^{(k)} | \Gamma_i P_i J_i M_i \rangle$ depends sensitively on the wave functions at short distances, while in the length form they depend sensitively on the wave functions at long distances [19,20]. The magnetic transition rates depend sensitively on the wave functions at intermediate distances.

III. RESULTS AND DISCUSSIONS

Figure 2 shows that our calculated $E2$ transition rates of ${}^2D_{5/2,3/2}^o \rightarrow {}^4S_{3/2}^o$ converge in a systematical and uniform manner with the increasing n_{\max} . In Fig. 2, the values in length and velocity form of ${}^2D_{5/2}^o \rightarrow {}^4S_{3/2}^o$ and ${}^2D_{3/2}^o \rightarrow {}^4S_{3/2}^o$ transition rates merge together at $n_{\max} = 9$. More specifically, the average values $\mathcal{A} = (\mathcal{A}^L + \mathcal{A}^V)/2$ of each transition rate vary about 1.1% from $n_{\max} = 8$ to $n_{\max} = 9$. Namely, for the ${}^2D_{5/2}^o \rightarrow {}^4S_{3/2}^o$ transition, $\mathcal{A}_{n_{\max}=8} = 3.99 \times 10^{-5} \text{ s}^{-1}$ and $\mathcal{A}_{n_{\max}=9} = 3.94 \times 10^{-5} \text{ s}^{-1}$; for the ${}^2D_{3/2}^o \rightarrow {}^4S_{3/2}^o$ transition, $\mathcal{A}_{n_{\max}=8} = 2.62 \times 10^{-5} \text{ s}^{-1}$ and $\mathcal{A}_{n_{\max}=9} = 2.59 \times 10^{-5} \text{ s}^{-1}$. For the two transitions, if we set $\mathcal{A}_{n_{\max}=9}$ as the “benchmark” values, respectively, the differences of the transition rates in length and velocity forms of $n_{\max} = 9$ compared with the benchmark values are all about 2.2%. In Chen’s calculations [6] the uncertainty of ${}^2D_{3/2}^o \rightarrow {}^4S_{3/2}^o$ transition rates ($3.48_{-0.99}^{+0.20} \times 10^{-5} \text{ s}^{-1}$) is much bigger than the uncertainty of ${}^2D_{5/2}^o \rightarrow {}^4S_{3/2}^o$ transition rates ($3.00_{-0.06}^{+0.06} \times 10^{-5} \text{ s}^{-1}$), which means their calculations do not converge uniformly since the core-excitation correlations are not considered. In addition, Fig. 2 shows that the Breit interaction reduces the $E2$ transition rates about 27% by comparisons between the values with and without considering Breit interactions. Namely, for the ${}^2D_{5/2}^o \rightarrow {}^4S_{3/2}^o$ transition $\mathcal{A}_{n_{\max}=9}$ changes from $5.41 \times 10^{-5} \text{ s}^{-1}$ (without Breit interaction) to $3.94 \times 10^{-5} \text{ s}^{-1}$ (with Breit interaction) and for the ${}^2D_{3/2}^o \rightarrow {}^4S_{3/2}^o$ transition $\mathcal{A}_{n_{\max}=9}$ changes from $3.49 \times 10^{-5} \text{ s}^{-1}$ (without Breit interaction) to $2.59 \times 10^{-5} \text{ s}^{-1}$ (with Breit interaction). In our calculations,

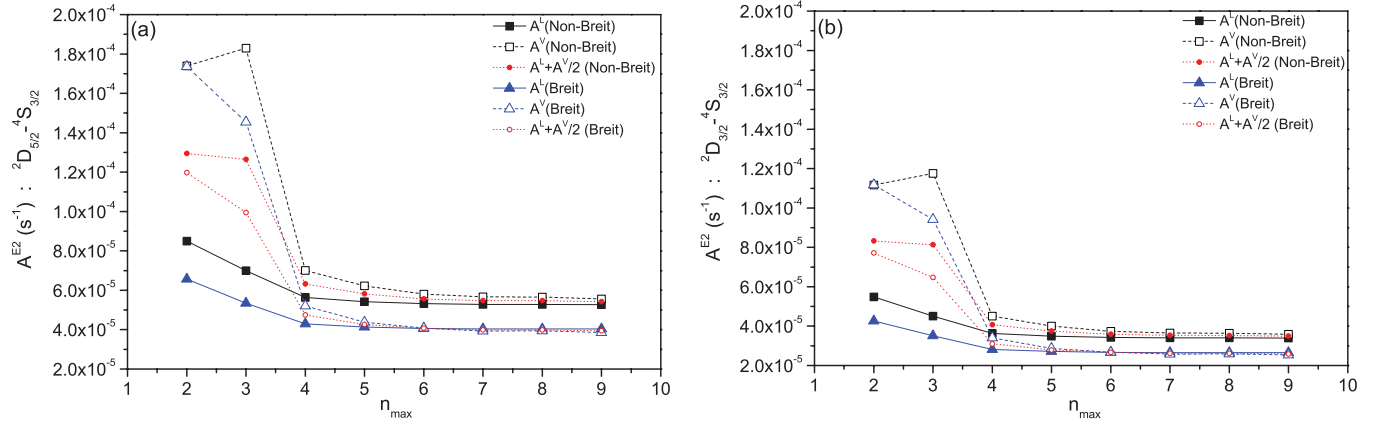


FIG. 2. (Color online) Our calculated $E2$ transition rates for ${}^2D_{5/2}^o \rightarrow {}^4S_{3/2}^o$ and ${}^2D_{3/2}^o \rightarrow {}^4S_{3/2}^o$ converge with the increasing n_{\max} of AO bases. Results of ${}^2D_{5/2}^o \rightarrow {}^4S_{3/2}^o$ transition are shown in panel (a) and results of ${}^2D_{3/2}^o \rightarrow {}^4S_{3/2}^o$ transition are shown in panel (b). \blacksquare , Results without considering the Breit interaction in length form; \square , results without considering the Breit interaction in velocity form; \blacktriangle , results considering the Breit interaction in length form; \triangle , results considering the Breit interaction in velocity form; \bullet , average value $\mathcal{A} = (\mathcal{A}^L + \mathcal{A}^V)/2$ without considering the Breit interaction; \circ , average value $\mathcal{A} = (\mathcal{A}^L + \mathcal{A}^V)/2$ considering the Breit interaction.

the rates of further considering the other QED corrections, for example, the vacuum polarization, the mass shift, and self-energy correlations, merely vary by a magnitude of about 0.001% compared with the results of only considering Breit interaction; hence, for clearer comparisons, we do not plot the results of taking into account the other higher-order QED corrections.

Figure 3 shows that our calculated $M1$ transition rates of ${}^2D_{5/2,3/2}^o \rightarrow {}^4S_{3/2}^o$ converge with the increasing n_{\max} . From $n_{\max} = 8$ to $n_{\max} = 9$, the $M1$ transition rates of ${}^2D_{5/2,3/2}^o \rightarrow {}^4S_{3/2}^o$ change 0.1%. This means that the $M1$ transition rates converge faster than $E2$ transition rates. In Fig. 3, it can be found that the Breit interaction affects the $M1$ transition rates by magnitude, which is more remarkable than the effect for $E2$ transition rates. This illustrates that the Breit (transverse) interaction represents especially the retarded magnetic interactions among the electron currents [17].

Table II shows our recommended $E2$ and $M1$ transition rates for ${}^2D_{5/2,3/2}^o \rightarrow {}^4S_{3/2}^o$ and the comparisons with other

theoretical values [4,6,12,13]. According to the convergence of the transition rates with the increasing n_{\max} , as shown in Figs. 2 and 3, the uncertainty of our recommended rates is given as 2.5% by considering the difference (2.2%) of the length and velocity form values and the difference (1.1%) between the values of $n_{\max} = 8$ and $n_{\max} = 9$. For the two transitions, in general, all the theoretical results with bigger values (e.g., $E2$ transition rates) agree better with each other than the tiny results (e.g., $M1$ transition rates). This demonstrates that achieving convergence of tiny values is more difficult.

In Table II, our calculated transition rates for ${}^2P_{3/2,1/2}^o \rightarrow {}^4S_{3/2}^o$ transitions are also listed. For the forbidden $M1$ transitions, the rates of ${}^2P_{3/2,1/2}^o \rightarrow {}^4S_{3/2}^o$ (in magnitude of 10^{-2}) are much larger than the rates of ${}^2D_{5/2,3/2}^o \rightarrow {}^4S_{3/2}^o$ (in magnitude of 10^{-4} and 10^{-6}), while for the forbidden $E2$ transitions, the rates of ${}^2D_{5/2,3/2}^o \rightarrow {}^4S_{3/2}^o$ (in magnitude of 10^{-5}) are larger than the rates of ${}^2P_{3/2,1/2}^o \rightarrow {}^4S_{3/2}^o$ (in magnitude of 10^{-6} and 10^{-8}). This is because of the favor of the angular momentum l transfers of one (two) for $M1$ ($E2$) transitions. That is to

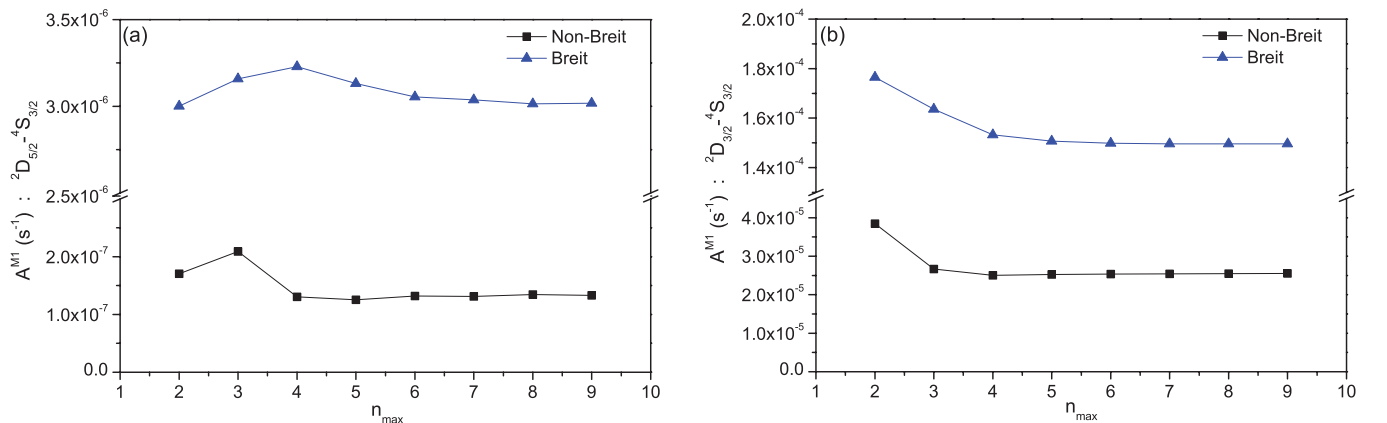


FIG. 3. (Color online) Our calculated $M1$ transition rates for ${}^2D_{5/2}^o \rightarrow {}^4S_{3/2}^o$ and ${}^2D_{3/2}^o \rightarrow {}^4S_{3/2}^o$ transitions converge with the increasing n_{\max} of AO bases. Results of the ${}^2D_{5/2}^o \rightarrow {}^4S_{3/2}^o$ transition are shown in panel (a) and results of the ${}^2D_{3/2}^o \rightarrow {}^4S_{3/2}^o$ transition are shown in panel (b). \blacksquare , Results without considering the Breit interactions; \blacktriangle , results considering the Breit interactions.

TABLE II. Our recommended $E2$ and $M1$ transition rates for ${}^2D_{5/2,3/2}^o \rightarrow {}^4S_{3/2}^o$ and the comparison with other theoretical values. Our calculated $E2$ and $M1$ transition rates for ${}^2P_{3/2,1/2}^o \rightarrow {}^4S_{3/2}^o$ (in unit of s^{-1}). The numbers in square brackets indicate the power of 10.

Transition	Type	This work ($n_{\max} = 9$)	Chen ^a	Zeippen ^b	Zeippen ^c	Fischer and Tachiev ^d
${}^2D_{5/2}^o \rightarrow {}^4S_{3/2}^o$	$E2$	$3.94^{+0.09}_{-0.09}[-5]$	$3.91^{+0.08}_{-0.11}[-5]$	$3.64[-5]$	$3.39[-5]$	$3.382[-5]$
	$M1$	$3.02^{+0.08}_{-0.08}[-6]$	$3.00^{+0.06}_{-0.06}[-6]$	$1.83[-6]$	$1.98[-6]$	$7.416[-6]$
	$E2 + M1$	$4.25^{+0.10}_{-0.10}[-5]$	$4.21^{+0.09}_{-0.11}[-5]$	$3.82[-5]$	$3.59[-5]$	$4.124[-5]$
${}^2D_{3/2}^o \rightarrow {}^4S_{3/2}^o$	$E2$	$2.59^{+0.06}_{-0.06}[-5]$	$3.48^{+0.20}_{-0.99}[-5]$	$2.36[-5]$	$2.20[-5]$	$2.209[-5]$
	$M1$	$1.50^{+0.04}_{-0.04}[-4]$	$1.48^{+0.01}_{-0.06}[-4]$	$1.41[-4]$	$1.59[-4]$	$1.414[-4]$
	$E2 + M1$	$1.75^{+0.05}_{-0.05}[-4]$	$1.83^{+0.03}_{-0.10}[-4]$	$1.65[-4]$	$1.81[-4]$	$1.635[-4]$
${}^2P_{3/2}^o \rightarrow {}^4S_{3/2}^o$	$E2$	$1.27^{+0.10}_{-0.10}[-6]$				$1.233[-8]$
	$M1$	$5.87^{+0.44}_{-0.44}[-2]$				$5.646[-2]$
	$E2 + M1$	$5.87^{+0.44}_{-0.44}[-2]$				$5.646[-2]$
${}^2P_{1/2}^o \rightarrow {}^4S_{3/2}^o$	$E2$	$5.27^{+4.16}_{-4.16}[-8]$				$1.510[-6]$
	$M1$	$2.35^{+0.18}_{-0.18}[-2]$				$2.265[-2]$
	$E2 + M1$	$2.35^{+0.18}_{-0.18}[-2]$				$2.265[-2]$

^aCalculations by Chen *et al.* [6].

^bCalculations by Zeippen [12].

^cCalculations by Zeippen [13].

^dCalculations by Fisher and Tachiev [4].

say the major contributions of the $M1$ transition mainly result from the transitions of ${}^2P_{3/2,1/2}^o$ terms to ${}^4S_{3/2}^o$ terms because of a favor of change one for l . We note that the ${}^2D_{3/2}$ state has a component of ${}^2P_{3/2}^o$ term since different LS coupling terms with the same total angular momentum J will mix due to the spin-orbit interactions, while the ${}^2D_{5/2}$ state has no ${}^2P_{3/2,1/2}$ components. Therefore, the $M1$ transition rate of ${}^2D_{3/2} \rightarrow {}^4S_{3/2}$ is much larger than that of ${}^2D_{5/2} \rightarrow {}^4S_{3/2}$. Although the absolute value of $M1$ transition rates of ${}^2D_{5/2,3/2} \rightarrow {}^4S_{3/2}$ are small, it is interesting to note that we still can calculate the $M1$ rates with enough accuracy because we have achieved enough convergence for the $E2$ transition rates. The uniform convergence guarantees the convergence of the products of the initial and final wave functions at large and small distances according to the $E2$ matrix elements of the length gauge and velocity gauge, respectively, and then ensures the $M1$ transition matrix elements with nearly the same accuracy, which involves the integrations at intermediate distances.

Similarly, for $E2$ transitions the major contributions mainly result from the transitions of ${}^2D_{5/2,3/2}^o$ terms to ${}^4S_{3/2}^o$ terms because of a favor of change of two for l . The ${}^2P_{3/2}^o$ state has a component of ${}^2D_{3/2}^o$ term due to the spin-orbit interactions, while the ${}^2P_{1/2}^o$ state has no mixture of ${}^2D_{5/2,3/2}^o$ terms; hence, the $E2$ transition rate of ${}^2P_{3/2}^o \rightarrow {}^4S_{3/2}^o$ should be much larger than that of ${}^2P_{1/2}^o \rightarrow {}^4S_{3/2}^o$. In Table II, the results of Fischer and Tachiev [4] are reversed, namely 1.233×10^{-8} for ${}^2P_{3/2}^o \rightarrow {}^4S_{3/2}^o$ and 1.510×10^{-6} for ${}^2P_{1/2}^o \rightarrow {}^4S_{3/2}^o$, which are unreasonable from the above qualitative analysis. Our results of 1.27×10^{-6} for ${}^2P_{3/2}^o \rightarrow {}^4S_{3/2}^o$ and 5.27×10^{-8} for ${}^2P_{1/2}^o \rightarrow {}^4S_{3/2}^o$ are reasonable. In our calculations, for $E2$ transition rates of ${}^2P_{3/2,1/2}^o \rightarrow {}^4S_{3/2}^o$, the uncertainties are larger than those of ${}^2D_{5/2,3/2}^o \rightarrow {}^4S_{3/2}^o$ transition rates since it is very difficult to calculate the tiny $E2$ rates of ${}^2P_{3/2,1/2}^o \rightarrow {}^4S_{3/2}^o$ transitions.

The uncertainty of the $E2$ transition rate of ${}^2P_{3/2}^o \rightarrow {}^4S_{3/2}^o$ is estimated as about 7.5%, which involves the difference between the results of length and velocity forms (about 7.5%) and the difference between the values of $n_{\max} = 8$ and $n_{\max} = 9$ (<1%). For the $M1$ transition rate of ${}^2P_{3/2}^o \rightarrow {}^4S_{3/2}^o$, the difference between the values of $n_{\max} = 8$ and $n_{\max} = 9$ is smaller than 1%, but we give the same uncertainty 7.5% as the uncertainty of the corresponding $E2$ transition rate. The $E2$ transition rate of ${}^2P_{1/2}^o \rightarrow {}^4S_{3/2}^o$ is tiny (in magnitude of 10^{-8}), the complete convergence of which may be affected by the numerical errors caused by present double precision calculations and is out of the scope of this work. For the $M1$ transition rate of ${}^2P_{1/2}^o \rightarrow {}^4S_{3/2}^o$, the difference between the values of $n_{\max} = 8$ and $n_{\max} = 9$ is smaller than 1%, but considering the uncertainty of the ${}^2P_{3/2}^o \rightarrow {}^4S_{3/2}^o$ transition and that ${}^2P_{3/2}$ and ${}^2P_{1/2}$ belong to the same LS term, here we still give the same uncertainty as 7.5%.

According to the recommended $E2$ and $M1$ transition rates, the recommended ratio between ${}^2D_{5/2}^o \rightarrow {}^4S_{3/2}^o$ and ${}^2D_{3/2}^o \rightarrow {}^4S_{3/2}^o$ transition rates in high-electron-density limit can be obtained by the following formula [1]:

$$r(\infty) = \frac{6\mathcal{A}^{(E2+M1)}({}^2D_{5/2}^o \rightarrow {}^4S_{3/2}^o)}{4\mathcal{A}^{(E2+M1)}({}^2D_{3/2}^o \rightarrow {}^4S_{3/2}^o)}. \quad (5)$$

Table III shows our recommended ratios (with uncertainty of 2.5%) and the comparisons with the measurements [9,10] and other theoretical values [1,6,12–14]. For clearer comparisons, all the values are plotted in Fig. 4.

Figure 4 shows that the previous calculated ratios change a lot from 0.43 to 0.26 from 1957 to 1996. Until to 1996, only two calculation results, Eissner in 1981 [2] and Zeippen in 1982 [12], are within the experimental uncertainties of Monk [10]. These two calculations are carried out on

TABLE III. The intensity ratio between ${}^2D_{5/2}^o \rightarrow {}^4S_{3/2}^o$ and ${}^2D_{3/2}^o \rightarrow {}^4S_{3/2}^o$ transition rates in the high-electron-density limit.

	This work	Chen [6]	Seaton [1]	Eissner [2]	Zeippen [12]	Zeippen [13]	Wiese [14]	Fisher & Tachiev [4]
Calculation (∞)	0.363 ± 0.009	$0.345^{+0.028}_{-0.014}$	0.43	0.35	0.348	0.297	0.26	0.378
	Monk [10]	Wang and Liu [9]						
Observation (∞)	0.339 ± 0.028	0.378 ± 0.017						

a set of small AO bases only considering five and nine configurations, respectively, and adopting a nonrelativistic Hamiltonian followed by relativistic corrections. It is noted that Zeippen's calculated transition rates for ${}^2D_{5/2,3/2}^o \rightarrow {}^4S_{3/2}^o$ [12] are lower than our calculated values, respectively, which means his calculations do not converge enough, although his ratio is within the measurement uncertainties. In 1987 Zeippen gave a new ratio value 0.297 [13] based on a new AO basis with $n_{\max} = 4$ including 23 configurations. The new ratio is lower than the lower limit of the measurements since his rate of ${}^2D_{5/2}^o \rightarrow {}^4S_{3/2}^o$ is lower and his rate of ${}^2D_{3/2}^o \rightarrow {}^4S_{3/2}^o$ is higher than the corresponding values given in 1982. Then Fisher and Tachiev, using the MCHF + BP method, present a ratio value 0.378 [4] within the measurement uncertainties of Wang and Liu [9]. Recently, Chen *et al.* carry out a large-scale MCDF calculation and give a ratio with a nonuniformity uncertainty, that is, $r(\infty) = 0.345^{+0.028}_{-0.014}$ [6]. In Chen's calculations the transition rates for ${}^2D_{5/2,3/2}^o \rightarrow {}^4S_{3/2}^o$ converge to a certain degree and his ratio with uncertainties has some overlap of two experimental uncertainties. However, since in Chen's calculations the transition rates for ${}^2D_{5/2}^o \rightarrow {}^4S_{3/2}^o$ and ${}^2D_{3/2}^o \rightarrow {}^4S_{3/2}^o$ do not converge uniformly, the uncertainties of his given ratio are bigger and nonuniform. In Fig. 4, the newest ratio, that is, $r(\infty) = 0.363 \pm 0.009$, is within the overlap range of two experimental measurements and with the smallest uncertainty, which means the present calculations converge enough and the large-scale MCDF calculation based on a set of quasicomplete basis is an efficient strategy.

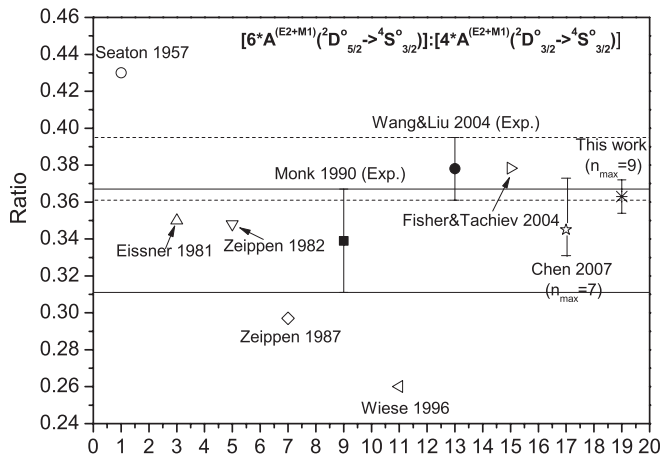


FIG. 4. The intensity ratio between ${}^2D_{5/2}^o \rightarrow {}^4S_{3/2}^o$ and ${}^2D_{3/2}^o \rightarrow {}^4S_{3/2}^o$ transition rates at the high-electron-density limit. The dashed lines are the upper and lower limits of Wang and Liu observations [9]. The solid lines are the upper and lower limits of Monk observations [10].

According to the calculated $E2$ and $M1$ transition rates, the ratio between ${}^2P_{3/2}^o \rightarrow {}^4S_{3/2}^o$ and ${}^2P_{1/2}^o \rightarrow {}^4S_{3/2}^o$ transition rates in high-electron-density limit can be obtained by

$$r(\infty) = \frac{4\mathcal{A}^{(E2+M1)}({}^2P_{3/2}^o \rightarrow {}^4S_{3/2}^o)}{2\mathcal{A}^{(E2+M1)}({}^2P_{1/2}^o \rightarrow {}^4S_{3/2}^o)}. \quad (6)$$

Our calculated ratio is $r(\infty) = 4.99 \pm 0.38$, which agrees with the ratio value (4.985) of Fisher and Tachiev [4]. This means that the large difference between our and Fisher and Tachiev's calculated $M1$ transition rates of ${}^2P_{3/2,1/2}^o \rightarrow {}^4S_{3/2}^o$ has nearly no effect on the ratio values since the $M1$ rates are smaller than the $E2$ rates by several orders.

Finally, we make the following conclusion. Based on a set of quasicomplete basis, a large-scale MCDF calculation is carried out and a systematical and uniform convergence is obtained. The converged forbidden $E2$ and $M1$ transition rates for (${}^2D_{5/2,3/2}^o \rightarrow {}^4S_{3/2}^o$) with 2.5% uncertainty by taking into account the large-scale electron correlations (including valence-excitation and core-excitation correlations) and QED corrections (especially the Breit interactions) are recommended. A ratio value for the two transitions of ${}^2D_{5/2,3/2}^o \rightarrow {}^4S_{3/2}^o$ in the limit of high-electron-density is given, that is, $r(\infty) = 0.363 \pm 0.009$. The recommended ratios as well as the transition rates for ${}^2D_{5/2,3/2}^o \rightarrow {}^4S_{3/2}^o$ are expected to be useful for astronomy and astrophysics. In addition, we note that the forbidden transition rates of different fine structure levels belonging to the same LS term can differ by 2 orders. We give a qualitative explanation from the physical picture why such an interesting phenomenon will happen. This explanation is useful for qualitatively testing the tiny values of the forbidden transitions. Furthermore, the $E2$ and $M1$ forbidden transition rates of ${}^2P_{3/2,1/2}^o \rightarrow {}^4S_{3/2}^o$ are given and the ratio value for the two transitions in the limit of high-electron-density is given, that is, $r(\infty) = 4.99 \pm 0.38$, which deserve further study.

ACKNOWLEDGMENTS

This work is supported by the National Basic Research Program (Grants No. 2010CB922900 and No. 2011CB921501), the National Science Foundation of China (Grants No. 10933001 and No. 10804012), Ministry of Science and Technology and Ministry of Education of China, the Key Grant Project of Chinese Ministry of Education (Grant No. 306020), Foundations for Development of Science and Technology of CAEP (Grant No. 2011A0102007), and the National Science and Technology Major Project of the Ministry of Science and Technology of China.

- [1] M. J. Seaton and D. E. Osterbrock, *Astrophys. J.* **125**, 66 (1957).
- [2] W. Eissner and C. J. Zeippen, *J. Phys. B* **14**, 2125 (1981).
- [3] G. I. Tachiev and C. F. Fischer, *Astron. Astrophys.* **385**, 716 (2002).
- [4] C. F. Fisher and Tachiev, *At. Data Nucl. Data Tables* **87**, 1 (2004).
- [5] Y. Zou and C. F. Fischer, *Phys. Rev. Lett.* **88**, 183001 (2002).
- [6] S. H. Chen, B. Qing, and J. M. Li, *Phys. Rev. A* **76**, 042507 (2007).
- [7] P. Jonsson, X. He, C. F. Fischer, and I. P. Grant, *Comput. Phys. Commun.* **177**, 597 (2007).
- [8] B. Qing, C. Cheng, X. Gao, X. L. Zhang, and J. M. Li, *Chin. Phys. Soc.* **59**, 145 (2010).
- [9] W. Wang, X. W. Liu, Y. Zhang, and M. Barlow, *Astron. Astrophys.* **873**, 886 (2004).
- [10] D. J. Monk, M. J. Barlow, and R. E. S. Clegg, *Mon. Not. R. Astron.* **242**, 457 (1990).
- [11] M. V. F. Copetti and B. C. Witzel, *Astron. Astrophys.* **382**, 282 (2002).
- [12] C. J. Zeippen, *Mon. Not. R. Astron. Soc.* **198**, 111 (1982).
- [13] C. J. Zeippen, *Astron. Astrophys.* **173**, 410 (1987).
- [14] W. L. Wiese, J. R. Fuhr, and T. M. Deters, *Atomic Transition Probabilities of Carbon, Nitrogen, and Oxygen: A Critical Data Compilation* (American Chemical Society, Washington, DC, 1996).
- [15] J. B. Mann and W. R. Johnson, *Phys. Rev. A* **4**, 41 (1971).
- [16] I. P. Grant and B. J. McKenzie, *J. Phys. B* **13**, 2671 (1980).
- [17] I. P. Grant, *Relativistic Quantum Theory of Atoms and Molecules* (Springer-Verlag, New York, 2006), Secs. 4.9 and 10.11.
- [18] I. Wenaker, *Phys. Scr.* **42**, 667 (1990).
- [19] I. P. Grant, *J. Phys. B* **7**, 1458 (1974).
- [20] Z. X. Zhao and J. M. Li, *Acta. Phys. Sin.* **34**, 1769 (1974).
- [21] K. G. Dyall *et al.*, *Comput. Phys. Commun.* **55**, 425 (1989).